Modification of endothelial nitric oxide synthase by 4-oxo-2(E)-nonenal(ONE) in preeclamptic placentas

Paul Guerby, Audrey Swiader, Oriane Tasta, Frédéric Pont, Frédéric Rodriguez, Olivier Parant, Christophe Vayssière, Takahiro Shibata, Koji Uchida, Robert Salvayre, et al.

Modification of endothelial nitric oxide synthase by 4-oxo-2(E)-nonenal(ONE) in preeclamptic placentas.

Paul Guerby[1,2*], Audrey Swiader[1*], Oriane Tasta[1,2], Frédéric Pont[3], Frédéric Rodriguez[4], Olivier Parant[2], Christophe Vayssière[2], Takahiro Shibata[5], Koji Uchida[6], Robert Salvayre[1], Anne Negre-Salvayre[1]

[1]Inserm U-1048, Université de Toulouse, France

[2]Pôle de gynécologie obstétrique, Hôpital Paule-de-Viguier, CHU de Toulouse, France

[3]Pôle technologique du CRCT, Toulouse, France

[4]SPCMIB UMR 5068 CNRS-UPS, Toulouse, France

[5] Graduate School of Bioagricultural Sciences, Nagoya University, Japan

[6]Laboratory of Food Chemistry, University of Tokyo, Japan

[*] Equally contributors

Running title :ONE-modified placental eNOS in preeclampsia

Corresponding author: Dr A. Negre-Salvayre INSERM U1048, BP84225, 31432 Toulouse Cedex 4 France. Tel. (33) 561-32-27-05 - Fax (33) 561-32-20-84

E-mail: anne.negre-salvayre@inserm.fr

Highlights

Lipid peroxidation products accumulate in placentas from preeclampsia

ONE-Lys adducts accumulate on eNOS in preeclamptic placentas

Recombinant eNOS is modified by ONE on Lys residues

ONE modifieseNOS and alters NO production in HTR8 trophoblasts

The migration of HTR8 inhibited by ONE is restored by the NO donor NOC-18

Key-words: Preeclampsia, placental eNOS, 4-oxo-2(E)-nonenal, 4-hydroxynonenal, acrolein, nitric oxide, trophoblasts, invasion

Abbreviations: PE, preeclampsia; LPP, lipid peroxidation products; ONE,4-oxo-2(E)-nonenal; NO, nitric oxide; eNOS, endothelial nitric oxide synthase; Lys (K), lysine;

ABSTRACT

Preeclampsia (PE) is a leading cause of pregnancy complications, affecting 3-7% of pregnant women worldwide.The pathophysiology of preeclampsia involves a redox imbalance, oxidative stress and a reduced nitric oxide (NO) bioavailability. The molecular and cellular mechanisms leading to the dysfunction of the placental endothelial NO synthase (eNOS) are not clarified. This study was designed to investigate whether aldehydes generated by lipid peroxidation products (LPP), may contribute to placental eNOS dysfunction in PE.

The analysis of placentas from PE-affected patients and normal pregnancies, showed a significant increase in protein carbonyl content, indicative of oxidative stress-induced protein modification,as shown by the accumulation of acrolein, 4-hydroxynonenal (HNE), and 4-oxo-2(E)-nonenal (ONE) adducts in PE placentas. In contrast, the levels of these LPP-adducts were low in placentas from normal pregnancies. Immunofluorescence and confocal experiments pointed out a colocalization of eNOS with ONE-Lys adducts, whereas eNOS was not modified in normal placentas. LC-MS/MS analysis of recombinant eNOS preincubated with ONE, allowed to identify several ONE-modified Lys-containing peptides, confirming that eNOS may undergo post-translational modification by LPP. The preincubation of HTR-8/SVneo human trophoblasts (HTR8) with ONE, resulted in ONE-Lys modification of eNOS and a reduced generation of NO. ONE inhibited the migration of HTR8 trophoblasts in the wound closure model, and this was partly restored by the NO donor, NOC-18, which confirmed the important role of NO in the invasive potential of trophoblasts.

In conclusion, placental eNOS is modified by ONE in PE placentas, which emphasizes the sensitivity of this protein to oxidative stress in the disturbed redox environment of preeclamptic pregnancies.

Introduction

Preeclampsia (PE) is a leading cause of pregnancy complications, affecting 3-7% of pregnant women worldwide [1-3]. The diagnosis of PE is suspected in case of *de novo* maternal hypertension (>140/90 mm Hg systolic/diastolic blood pressure) and proteinuria (>300 mg/24 h), observed after 20 weeks ofgestation. If untreated, PE evolves towards complications of eclampsia and HELLP syndrome (Hemolysis, Elevated Liver enzymes and Low Platelet count), kidney injury and acute respiratory distress syndrome [1-5]. The complications of PE may affect both the mother and the foetus, with an increased risk of fetal growth restriction, preterm birth, placental abruption, maternal and fetal mortality [2,3].The clinical symptoms are alleviated with the delivery, but PE could increase the risk of developing cardiovascular diseases, type 2 diabetes, or cancers [5-8].

Reactive oxygen species (ROS) are physiologically generated during placentation and throughout pregnancy [9-13]. During the early stages of pregnancy, the normal placentation requires a local low pO_2 environment allowing the invasion and plug of spiral arteries by cytotrophoblasts [12,13]. These conditions of relative hypoxia may prevent oxidative damages to the embryo which has low levels of antioxidant defenses in the first stages of development [14]. At the end of the first trimester, trophoblastic plugs are progressively degraded, and spiral arteries are remodeled into low resistance vessels, allowing the passage of maternal blood in the placental intervillous chamber and the progressive increase of placental pO_2 [14,15]. A number of factors including angiogenic growth factors, estrogens, or vasodilator mediators (nitric oxide, hydrogen sulfide), are involved in the remodeling of spiral arteries and placentation [10,14,15].

The pathophysiology of PE involves a defective trophoblastic invasion to the spiral arteries, resulting in abnormal placentation and disturbed maternal uteroplacental blood flow with abnormal conditions of hypoxia/oxygenation [9,10,13-15]. These events generate a redox imbalance and oxidative stress, as well as inflammation and release in the maternal blood of cytokines and placental-derived antiangiogenic factors (soluble fms-like tyrosine kinase-1, soluble endoglin), that generate endothelium dysfunction [16-18]. The causes of defective placentation could involve a

reduced bioavailability of nitric oxide (NO) for which several possible mechanisms have been reported, including a reduced expression and polymorphism of placental eNOS, or a depletion in arginine or in tetrahydrobiopterin (BH4), leading to eNOS uncoupling and dysfunction [10,19-21]. In the vascular wall, the activity of eNOS is regulated by post-translational modifications, including acylation, phosphorylation, S-nitrosylation or S-glutathionylation, depending on the cellular redox state[22]. We recently reported that placental eNOS is highly S-glutathionylated in preeclamptic patients, probably consequently to oxidative stress [23].

At the cellular level, oxidative stress induces damages on lipids, proteins and DNA, causing endoplasmic reticulum stress, cellular dysfunction and cell death [24-26]. Proteins can be damaged by ROS, *via* a direct oxidation of amino acid residues, and indirectly *via* their modification by lipid oxidation products (LPP) [25,27-30]. The oxidation of polyunsaturated fatty acids (PUFAs) generates many LPP, including aldehydes such as acrolein, 4-hydroxynonenal (HNE), malondialdehyde (MDA), or 4-oxo-2-nonenal (ONE). These LPP covalently bind to the nucleophilic sulfhydryl and primary amine groups of proteins, forming Schiff bases, Michael adducts and protein crosslinks [31-34]. Several proteins can be targeted by LPP, particularly lipoproteins, serum albumin, growth factor receptors, mitochondrial and extracellular matrix proteins, with consequences depending on their local concentration, the nature of stressors, cell type, oxidative stress intensity and duration [35-37). LPP-adduct formation triggers various biological responses, ranging from hormesis and the induction of protective mechanisms at low concentrations, to "carbonyl stress" characterized by protein dysfunction, inflammatory responses, accelerated senescence and toxic events [30,34-38].

HNE- and MDA-adducts are detected in the fetal and maternal circulation, in syncytiotrophoblasts, in endothelial cells and macrophages from pathological pregnancies [38-40], suggesting their possible involvement in fetal and maternal endothelial dysfunction and complications [37,38]. As LPP may inhibit NOS activity and reduce NO generation in vascular cells, [38,41,42], we investigated whether LPP may affect placental eNOS activity, with possible consequences on PE pathophysiology.

Materials and Methods

Materials

Anti-eNOS (ab5589) used for immunohistochemistry, anti-acrolein (ab48501) and ONE were from Abcam (Paris, France). Anti-4-HNE Michael adduct antibody (24327) was purchased from Oxis Research (Tebu-Bio, France). The anti-ONE-lysine antibody was prepared as reported [43]. Recombinant eNOS was from Enzo-Life Science (Villeurbanne, France). Secondary Alexa Fluor antibodies (488 and 546) were from Life Technologies (Courtaboeuf, France). DAF-FM diacetate (4-amino-5-methylamino-2',7'-difluorofluorescein diacetate), VEGF and DAPI (4,6-Diamidino 2-phenylindole dihydrochloride) were from Sigma-Aldrich (Saint Quentin Fallavier, France). NOC-18 (diethylene-triamine/nitric oxide adduct; DETA NONOate) was from Santa Cruz Biotechnology (Clinisciences, France).

Placental Tissue Collection

Human placentas were recovered through caesarean delivery (University Hospital Center of Toulouse, France) and analyzed upon approval by the Research Ethic Committee of Toulouse Hospitals (CER number 03-0115), as reported [23]. Two groups of placentas were analyzed, one group from normotensive pregnant women (n=9), one with severe and very severe PE features (n=13). PE parameters were defined according to the American College of Obstetricians and Gynecologists as the presence of a systolic blood pressure (SBP) higher than or equal to 140 mm Hg, or a diastolic blood pressure (DBP) higher than or equal to 90 mm Hg and a proteinuria higher than or equal to 300 mg per 24-hours urine collection after 20 weeks of gestation.

Immediately after their recovery, placentas were carefully rinsed in ice-cold PBS, one sample was fixed into 4% paraformaldehyde for immunofluorescence analysis. Another sample was kept frozen at -80°C until use. Placental homogenates for biochemistry analysis, were prepared as described [23].

Cell culture and cell viability

HTR-8/SVneo cells (HTR8) were a generous gift from Dr. Charles Graham (Kingston, Canada), and were cultured in RPMI supplemented with 5% fetal bovine serum (FBS) (5% CO_2, 20% O_2, 37°C) [44]. Before experiments, subconfluent HTR8 were incubated in FBS-free RPMI *w/wo* aldehydes, as indicated in the text and legends to figures, and put in a hypoxic chamber (5% CO_2, 1% O_2, 37°C), as reported [23]. Cell viability was estimated using the MTT [3-(4,5dimethylthiazol-2-yl)-2,5-diphenyltetrazolium bromide] assay.

Carbonylated protein content

The carbonylated protein content was measured using the Protein Carbonyl ELISA kit (Enzo LifeSciences, Villeurbanne, France) according to the instructions of the manufacturer. The absorbance was read at 450 nm (spectrophotometer microplate reader TECAN France).

Immunofluorescence studies

Immunofluorescence experiments were carried out on 3 µm thin sections of placentas. The accumulation of aldehyde-adducts and the modification of placental eNOS were evaluated by co-immunostaining experiments using as primary antibodies, anti-human eNOS polyclonal rabbit antibody, anti-ONE-lysine monoclonal [43], anti-acrolein monoclonal, or anti HNE-adduct monoclonal mouse antibodies, and secondary anti-mouse Alexa fluor-488 and anti-rabbit Alexa fluor-546-conjugated antibodies. Nuclei were stained with DAPI (1 µg/mL). The slides were analyzed by confocal microscopy (Zeiss LSM780). The percentage of eNOS overlapping with aldehydes was determined using the plug-in JACoP of ImageJ software, by evaluating the Mander's coefficient [45].

Wound closure assay

The invasive potential of HTR8 was evaluated by the wound closure assay, as reported [23]. Confluent HTR8 were preincubated for 2 hours with HNE 10 µM or ONE 1µM. A scratch was made

with a pipette tip, the medium was replaced by fresh FBS-free medium containing (or not) the NO donor NOC-18 (5 µM), and cells were put in a hypoxic chamber (1% O_2) for 48h as reported [23]. At the end, cells were fixed with 4% paraformaldehyde, and permeabilized for 5 min with 0.25% Triton X-100 in PBS, DAPI-stained and observed by fluorescence microscopy.

Determination of NO production by HTR8 trophoblasts

The production of NO by HTR8 was determined with the DAF-FM diacetate probe (5 µM), in the conditions given by the manufacturer [23]. Alternatively, eNOS activity was determined by measuring the nitrite/nitrate production, using the Nitric oxide Synthase activity Assay kit (Abcam, France).

Mass spectrometry

Recombinant human eNOS (ALX-201-853, 1µg) (Enzo LifeSciences, Villeurbanne, France) was modified by ONE (1 mM, overnight at 37°C) [46].

eNOS in-solution digestion. eNOS samples were dried in a concentrator and digested overnight at 37°C with 400 ng of sequencing-grade porcine trypsin (Promega) diluted in 20 µL of NH_4HCO_3 (100 mM). Peptides were dried and diluted in 10% acetonitrile 0.05% TFA before injection in LC-MS run.

eNOS LC-MS analysis. The peptides digested from eNOS were measured on an SCIEX 5600+ TripleTOF mass spectrometer operated in DDA mode. A Dionex Ultimate 3000 nanoLC HPLC system and a Hypersil GOLD 150x0.32 mm column (Thermo Scientific), packed with C18 3 µm 175 Å material, were used for peptide separation. For the HPLC method, the buffer A used was 0.1% (v/v) formic acid, and the buffer B was 0.1% (v/v) formic acid, 90% (v/v) acetonitrile. The gradient was 4–45% of buffer B in 24 min with a flow rate of 5 µL/min. For MS method, a survey scan at the MS1 level (350–1600 m/z) was first carried out with 250 ms per scan. The Top20 most intense precursors, whose charge states are 2–4 were fragmented. Signals exceeding 75 counts per second were selected for fragmentation and MS2 spectra generation. MS2 spectra were collected in the mass range 100–1600 m/z for 80 ms per scan. The dynamic exclusion time was set to 10 s.

LC-MS data analysis. To identify eNOS peptides, profile-mode.wiff files from data acquisition were centroided and converted to mzML format using the AB Sciex Data Converter v.1.3 and submitted to Mascot [47] (version 2.5) database searches against UniProtSwiss-Prot human database [48]. ESI-Quad-TOF was chosen as the instrument, trypsin/P as the enzyme and 2 missed cleavages were allowed. Peptide tolerances at MS and MS/MS level were set to be 20 ppm and 0.2 Da, respectively. Peptide variable modifications allowed during the search are shown in Table I. To calculate the false discovery rate (FDR), the search was performed using the "decoy" option in Mascot.

Table I

Name	Delta mass
4-ONE (K)	154,09938
4-ONE+Delta:H(-2)O(-1)(K)	136,088815

Peaks heights of peptides MS1 spectra were measured using the Proline v2.0 software (http://www.profiproteomics.fr/proline/). The percentage of modified peptide on total peptide was calculated by the ratio of the cumulative peak heights of modified peptide peaks on the sum of all peptide heights (modified + unmodified) x100. These data are given as indicative because peptide modification by ONE can affect the peptide sensitivity and induce a missed cleavage.

In silico studies

The RX structures of NOS isozymes (neuronal nNOS from rat and inducible iNOS from human) were obtained on the PDB (http://www.rcsb.org/) database [49]. The endothelial NOS (eNOS, human) structures were issued from ModBase, a database of comparative protein structure models [50]. Two homology models of eNOS (using 1TLL PSB structure [51] as template) were available on ModBase, model 7e09b (short form of 7e09b90c4f6474771f6bc4e8d2370945) was chosen. Molecular graphics were performed with the UCSF Chimera package [52]. Chimera (http://www.rbvi.ucsf.edu/chimera/) is developed by the Ressource for Biocomputing, Visualization, and Informatics at the University of

California, San Francisco (supported by the NIGMS P41-GM103311). The protein structures (1TLL [50], 3HR4[52]), used in this paper were structurally aligned using UCSF Chimera/Matchmaker program [53].The PDB structure 1TLL (chain A) was chosen as reference for the structural set (1TLL [50], 3HR4 [52], model 7e09b) of eNOS reductase domain. The PDB structure 4D1O (chain A) was chosen as reference for the structural set (4D1O [54], 5VVD [55]) of eNOS oxygenase domain. The protein structures were prepared (structure checks, chain splitting) using Accelrys (Discovery Studio Modeling Environment, Release 4.0, San Diego: Accelrys Software Inc., 2013) Discovery Studio Visualizer 4.0 (DSV) and UCSF Chimera.

Statistical analysis

The results are expressed as mean ± SEM. For normally distributed data, Student's t-test was used, otherwise nonparametric Mann-Whitney U-test was employed. Statistical calculations were carried out using the software Graphpad Prism, version 6.01 (Graph Pad Software Inc., CA, USA). A p-value <0.05 was considered to indicate statistical significance.

Results

Accumulation of lipid oxidation-derived aldehydes in PE placenta

The detection of protein-adducts implicating aldehydes generated through the peroxidation of polyunsaturated fatty acids, is a hallmark of oxidative stress [30,56], which led us to check whether such adductscould be detected in the placentas of PE-affected women, as reported [38]. As shown in Fig.1A, a significant increase in carbonylated protein content was observed in homogenates from PE placentas, indicative of an amino-acid modification by reactive carbonyl compounds [56,57]. Immunofluorescence staining and confocal microscopy studies pointed out a strong accumulation of HNE-, acrolein- and ONE-aldehyde adducts in PE placentas, by comparison with placentas from normal pregnancies(Fig.1B and 1C).

Modification of eNOS by lipid oxidation products

Several evidences indicate that oxidative stress is associated with eNOS uncoupling or decreased expression, leading to its dysfunction [38,41]. However, whether LPP could alter eNOS activity is not known [38]. As various post-translational modifications may regulate eNOS activity [22], we checked whether LPP may modify eNOS.

Immunofluorescence and confocal microscopy studies highlighted a significant and strong modification of eNOS by ONE on Lys residues, (using an anti-ONE-Lys mAb [43]) in PE placentas (Fig.2, lower right panel). The modification of eNOS by HNE, was much weaker, though significant, and acrolein-adducts were not detected (Fig.2, upper and middle right panels), though both HNE- and acrolein-adducts were abundantly expressed in PE placentas (Fig1B,C). The modification of eNOS by LPP was low in placentas from normal pregnancies(Fig.2, left panels). No variation in total eNOS expression was observed between normal and PE placentas (Supp. Fig.I), as previously reported [23]. These immunofluorescence findings indicate that ONE forms adducts on placental eNOS in PE pregnancies. To confirm that ONE-adducts can be formed on eNOS and to identify which Lys residues could be targeted, MS studies were carried out on ONE-modified recombinant eNOS.

LC-MS/MS analysis of recombinant eNOS modified by ONE-

Recombinant human eNOS (1 µM) was incubated with ONE (1 mM, overnight at 37°C), prior to proteolytic digestion and liquid chromatography–tandem mass spectrometry (LC–MS/MS) analysis. Modified peptides were detected by LC–MS and their primary sequence was determined by MS/MS. In contrast to unreacted eNOS, the MS analysis of tryptic peptides from ONE-incubated eNOS allowed to identify several ONE-modified Lys(K) residues, in the oxygenase and reductase domains, the sequences being confirmed by MS/MS spectra (Fig.3A and Supp. Fig.II).

The modification of recombinant eNOS by ONE, significantly reduced its enzymatic activity (Fig.3B), so that we used molecular modelling to predict the three-dimensional structure of eNOS and the location of ONE-modified Lys-residues (Fig.3C). This 3D-modelling allowed to predict that most ONE-modified Lys-residues are located at the surface of the reductase and oxidase domains, and that at least two Lys-residues, K519 and K1085, could modulate eNOS activity. Lys(K)519 is located near the calmodulin (CaM)-binding domain [58], which suggests that its modification by ONE may alter the Ca^{2+} and CaM-dependent activation of the enzyme. Beside, Lys(K)1085 is located near the FAD/NADPH-containing domain [59], so that its modification by ONE could alter the transfer of electrons between the flavins, and inhibit enzyme activity (Fig.3C).

ONE alters the production of NO by HTR8 human trophoblasts

The effects of ONE were investigated on eNOS activity and NO production in cultured HTR8 human trophoblasts [44]. HTR8 were incubated under hypoxic conditions (1% O_2), in FBS-free medium, these conditions being convenient to evaluate HTR8 proliferation and migration [23]. Immunofluorescence and confocal microscopy analysis elicited on HTR8 (after 2h preincubation with ONE, 1 µM), allowed to detect the presence of ONE-adducts, particularly on eNOS (Fig.4A). These conditions generated a significant decrease in NO production (Fig.4B), and of eNOS enzymatic activation by VEGF (10 ng/mL) (Fig.4C). The preincubation of HTR8 with ONE did not elicit any loss of viability, up to 72h incubation in hypoxia (data not shown).

ONE inhibits the migration of HTR8 in the wound closure assay. Restoration by NOC-18

We then investigated whether ONE affects the invasive potential of HTR8 trophoblasts in the wound closure assay, and the role of NO. Under standard conditions, HTR8 maintained in low pO_2 conditions (1% O_2), and in serum-free medium, migrated within the wound (Fig.5, upper panel). In contrast, the migration of HTR8 was significantly inhibited when cells were preincubated with ONE, under conditions inhibiting NO production (Fig.5). The NO-donor, NOC-18 (5 µM) [60], significantly restored the migration of HTR8 exposed to ONE, thereby emphasizing the role of NO in the invasive potential of trophoblasts, in agreement with [23].

Altogether, these data indicate that ONE exogenously added to HTR8 culture medium, form Lys-adducts on eNOS, this resulting in a decreased NO production and altered trophoblast migration. These data support the hypothesis that ONE-Lys adducts generated on eNOS in PE placentas, could locally contribute to its dysfunction, with possible consequences on the invasive capacity of cytotrophoblasts and throughout pregnancy.

Discussion

NO produced by placental eNOS plays a key-role throughout pregnancy, whether in the early stages of placentation, trophoblast invasion and spiral artery remodeling, in embryo development, in the maternal/foetal vascular tone, and in the vasculogenic and angiogenic signalling evoked by growth factors (VEGF, TGFβ, angiopoietin-1/2...) and their receptors [61]. A close relationship has been established between oxidative stress and the decreased NO bioavailability which characterizes the pathophysiology of PE, with consequences on systemic endothelial dysfunction [10,12,62]. We recently reported that eNOS undergoes high levels of S-glutathionylation in PE placentas [23], a mechanism linked to oxidative stress and known to trigger eNOS uncoupling and reduced NO production [63]. In the present article, we show that eNOS undergoes post-translational modifications elicited by the highly reactive lipid oxidation-derived aldehyde ONE, in PE placentas

and in cultured HTR8 trophoblasts, with consequences on NO production and the invasive potential of trophoblasts.

A first observation is that PE placentas exhibit high levels of carbonyl proteins, a hallmark of oxidative stress and lipid peroxidation[27,30,56]. The carbonylation of proteinsresults from their irreversible post-translational modification by reactive carbonyl compounds (ketones, aldehydes), generated through lipid peroxidation, this resulting in protein dysfunction, or "carbonyl stress" [56,64]. Carbonyl stress links oxidative stress to disease progression and age-related disorders, that are associated with increased levels of carbonylated proteins [65]. As a matter of fact, the increased carbonyl protein level detected in PE placentas, may play a role in the premature senescence of this tissue, in agreement with recent evidence showing a role for oxidative stress in premature placental aging and PE pathophysiology [66]. Confocal microscopy pictures of PE placentas emphasized the abundant accumulation of ONE-, HNE- and acrolein-adducts, in agreement with previous reports showing an increased staining of HNE- and MDA-adducts in placentas from pathological pregnancies, in syncytiotrophoblasts, endothelial cells and macrophages [37,38,67,68], together with other features of oxidative stress, including an imbalance of the GSH/GSSG content, protein glutathionylation [23], and decreased activities of antioxidant enzymes (SOD, catalase, glutathione peroxidase) [10,38,69].

The post-translational modification of proteins by aldehyde-adducts may (or not) induce their dysfunction, with gain or loss of activity, depending on protein abundance, subcellular location, accessibility, and the nature of the modified residues [56]. Baraibar et al [65] recently identified more than 183 cellular and extracellular proteins susceptible to be carbonylated, in the cytosol, mitochondria, and at the plasma membrane. In the present study, we show that placental eNOS is a target of carbonyl stress, as assessed by confocal microscopy showing its colocalization with ONE-Lys adducts. Supporting this observation, thestructural analysis of recombinant eNOS confirmed that ONE may bind several Lys-residues. Surprisingly, we did not find any modification of Cys residues by ONE, whereas Cys is a target of ONE [70], and several Cys can be modified by S-glutathionylation

[23,63]. Anyway, ONE-Lys adducts generated on recombinant eNOS, should affect its enzymatic activity. Indeed, the 3D-modelling of eNOS shows that two Lys residues modified by ONE are close the Ca_2^+-calmodulin (K519), or the FAD/NADPH (K1085) domains, which may alter the enzymatic activity of recombinant eNOS. As a matter of fact, the addition of ONE to HTR8 trophoblasts, resulted in a decreased production of NO by these cells, and a decreased eNOS activity, that could partly result from the formation of ONE-Lys adducts on eNOS (Fig.4A). To our knowledge, this is the first report showing that eNOS is targeted by LPP, more precisely ONE, in addition to its previously reported post-translational modifications, including phosphorylation, nitrosylation, ubiquitination, sumoylation, glutathionylation, that may regulate the activity of neuronal, endothelial or inducible NOS [22,71]. Interestingly, a modification of eNOS by carbonyl stress was observed by Du et al [72], who reported that high glucose levels inhibit eNOS activity in BAEC and in the aorta of diabetic rats, *via* an *O*-linked N-acetylglucosamine post-translational modification at the Akt site, impairing the phosphorylation and activation of eNOS. Placental eNOS is exposed to redox variations occurring throughout pregnancy, particularly in PE, in which altered trophoblast invasion and defective placentation lead to ischemia/reperfusion waves, and massive ROS production [9,10,12,13,62]. S-glutathionylation of eNOS induces its uncoupling which converts its activity in a ROS generating enzyme that may contribute to locally increase oxidative stress, lipid peroxidation and the generation of LPP, able to rapidly react on proteins (including eNOS itself) or its substrates (Arginine).

Though HNE- and acrolein-adducts were detected in PE placentas, our data indicate that eNOS is only slightly modified by these LPP. This is in agreement with report from Whitsett et al, showing that the inhibitory effect of HNE on eNOS is not attributed to the modification of eNOS residues, but rather to the depletion in BH4 and/or an inhibition of serine 1179 phosphorylation on eNOS [41]. Previous studies have shown that ONE is much more reactive than HNE on protein nucleophiles, particularly on Lys, as it rapidly forms readily reversible Schiff base adducts on Lys, that can be oxidized to stable 4-ketoamide adducts for longer time of exposure [70,73-75]. ONE shares structural similarities with HNE, of which it differs by the carbonyl group in C4 position (instead of the hydroxyl group in HNE)

[73], which increases its cross-linking potential, and particularly the formation of Lys–Lys cross-links, thus it is considered as more reactive and more toxic than HNE [57,70,73,74].

The modification of eNOS by ONE triggers its dysfunction, as reported for other protein targets, such as an inhibition of tubulin polymerization [75], α-synuclein oligomerization [57],or the formation of adducts on histones [76]. In our study, the exposure of HTR8 to exogenous ONE inhibited their invasive capacity to migrate in the wound closure model, *via* mechanisms possibly resulting (at least in part), from eNOS modification and subsequent decreased NO production, since the NO donor NOC-18, significantly restored cell migration. Various NO-mediated signaling mechanisms have been shown to play a role in the invasive potential of trophoblasts. For instance, NO regulates the expression and activity of matrix metalloproteases (MMP2), which stimulate the migration and proliferation of human trophoblasts, including in HTR8 [77,78]. NO, cGMP and Sildenafil (an inhibitor of phosphodiesterase 5) promote the switching of trophoblast integrins from a stationary (α6β4) to a more invasive (α1β1) phenotype, which is an important step for initiating trophoblast invasion during placentation [79,80]. Likewise, NO and cGMP regulate the expression of growth factors such as HGF, an essential factor of placentation and trophoblast invasion [81], and VEGF which, beside its implication in vasculogenesis and angiogenesis, may contribute to trophoblast motility [82].

Our data confirm the role of NO in trophoblast invasiveness, and emphasize oxidative stress as a cause of post-translational modification of eNOS, by S-glutathionylation [23], and by lipid peroxidation-derived aldehydes such as ONE, which finally reduces NO production, thereby contributing to aggravate the pathological process of PE.

Acknowledgements

The authors wish to thank Pr. Charles H. Graham (Queen's University, Ontario, Canada), for giving us the HTR8/svNeo cytotrophoblast cell line. The cell Imaging Facility at INSERM U1048-I2MC and Proteomics platform (PôleTechnologique du CRCT) are gratefully acknowledged.

Fundings

This work was supported by INSERM (Institut National de la Santé et de la Recherche Médicale), and University Paul Sabatier Toulouse.

Declarations of interest: none

References

1. Roberts JM, Bell MJ. If we know so much about preeclampsia, why haven't we cured the disease? *Reprod Immunol.* 2013;99: 1–9.
2. Phipps EA, Thadhani R, Benzing T, Karumanchi SA. Pre-eclampsia: pathogenesis, novel diagnostics and therapies. *Nat RevNephrol*. 2019. doi: 10.1038/s41581-019-0119-6.
3. Uzan J, Carbonnel M, Piconne O, et al. Pre-eclampsia: pathophysiology, diagnosis, and management. *Vasc Health Risk Manag.*2011;7:467-74
4. Arulkumaran N, Lightstone L. Severe pre-eclampsia and hypertensive crises. *Best Pract Res Clin ObstetGynaecol.* 2013;27(6):877-84.
5. Garovic VD, Hayman SR. Hypertension in pregnancy: an emerging risk factor for cardiovascular disease. *Nat Clin PractNephrol*. 2011;3(11):613-22.
6. Brown MC, Best KE, Pearce MS, et al. Cardiovascular disease risk in women with pre-eclampsia: systematic review and meta-analysis. *Eur J Epidemiol.*2013;28(1):1-19.
7. Veerbeek JH, Hermes W, Breimer AY, et al. Cardiovascular disease risk factors after early-onset preeclampsia, late-onset preeclampsia, and pregnancy-induced hypertension. *Hypertension*. 2015;65:600-6.
8. Ahmed R, Dunford J, Mehran R, Robson S, Kunadian V. Pre-eclampsia and future cardiovascular risk among women: a review. *J Am Coll Cardiol*. 2014;63(18):1815-22.
9. Wu F, Tian FJ, Lin Y, Xu WM. Oxidative Stress: Placenta Function and Dysfunction. *Am J Reprod Immunol*. 2016;76(4):258-71.
10. Aouache R, Biquard L, Vaiman D, Miralles F. Oxidative Stress in Preeclampsia and Placental Diseases. *Int J Mol Sci*. 2018;19(5).
11. Sánchez-Aranguren LC, Prada CE, Riaño-Medina CE, Lopez M. Endothelial dysfunction and preeclampsia: role of oxidative stress. *Front Physiol*. 2014;5:372.
12. Jauniaux E, Poston L, Burton GJ. Placental-related diseases of pregnancy: Involvement of oxidative stress and implications in human evolution. *Hum Reprod Update*. 2006;12(6):747-55.
13. Jauniaux E, Hempstock J, Greenwold N, Burton GJ. Trophoblastic oxidative stress in relation to temporal and regional differences in maternal placental blood flow in normal and abnormal early pregnancies. *Am J Pathol*2003;162:115—25
14. Burton GJ, Woods AW, Jauniaux E, Kingdom JC. Rheological and physiological consequences of conversion of the maternal spiral arteries for uteroplacental blood flow during human pregnancy. *Placenta*. 2009;30(6):473-82.
15. Jauniaux E, Pahal GS, Gervy C, Gulbis B. Blood biochemistry and endocrinology in the human fetus between 11 and 17 weeks of gestation. *Reprod Biomed On-line*2000;1:38—44.
16. Kendall R, Thomas K. Inhibition of vascular endothelial cell growth factor activity by an endogenously encoded soluble receptor. *Proc NatlAcadSci USA* 1993 ;90:10705-10709.
17. Maynard SE, Min JY, Merchan J, et al. Excess placental soluble fms-like tyrosine kinase 1 (sFlt1) may contribute to endothelial dysfunction, hypertension, and proteinuria in preeclampsia. *J Clin Invest.* 2003;111(5):649-58.
18. Tjoa ML1, Levine RJ, Karumanchi SA. Angiogenic factors and preeclampsia. *Front Biosci*. 2007;12:2395-402.
19. Johal T, Lees CC, Everett TR, Wilkinson IB. The nitric oxide pathway and possible therapeutic options in pre-eclampsia. *Br J Clin Pharmacol*. 2014;78(2):244-57.
20. Lyall F, Bulmer JN, Kelly H, Duffie E and Robson SC Human trophoblast invasion and spiral artery transformation – The role of nitric oxide. *Am J Pathol*. 1999;154,1105–1114.
21. Lowe DT. Nitric oxide dysfunction in the pathophysiology of preeclampsia. *Nitric Oxide*. 2000;4(4):441-58.
22. Heiss EH, Dirsch VM. Regulation of eNOS enzyme activity by posttranslational modification. *Curr Pharm Des.* 2014;20(22):3503-13.

23. Guerby P, Swiader A, Augé N, Parant O, Vayssière C, Uchida K, Salvayre R, Negre-Salvayre A. High glutathionylation of placental endothelial nitric oxide synthase in preeclampsia. *Redox Biol*. 2019;22:101126. doi: 10.1016/j.redox.2019.101126.
24. Halliwell B. Biochemistry of oxidative stress. *Biochem Soc Trans*, 2007, 35:1147–1150.
25. Stadtman ER, Levine RL. 2003. Free radical-mediated oxidation of free amino acids and amino acid residues in proteins. *Amino Acids* 25:207–218.
26. Panieri E, Gogvadze V, Norberg E, Venkatesh R, Orrenius S, Zhivotovsky B. Reactive oxygen species generated in different compartments induce cell death, survival, or senescence. *Free Radic Biol Med*. 2013;57:176-87
27. Levine RL, Stadtman ER. 2001. Oxidative modification of proteins during aging. *Exp Gerontol* 36:1495–1502.
28. Castro JP, Jung T, Grune T, Siems W. 4-Hydroxynonenal (HNE) modified proteins in metabolic diseases. *Free Radic Biol Med*. 2017;111:309-315.
29. Forman HJ, Ursini F, Maiorino M. An overview of mechanisms of redox signaling. *J Mol Cell Cardiol*. 2014;73:2-9.
30. Dalle-Donne I, Giustarini D, Colombo R, Rossi R, Milzani A. Protein carbonylation in human diseases. *Trends Mol Med*. 2003;9(4):169-76
31. Esterbauer H, Schaur RJ, Zollner H. Chemistry and biochemistry of 4-hydroxynonenal, malonaldehyde and related aldehydes. *Free Radic Biol Med*. 1991;11(1):81-128.
32. Uchida K. Current status of acrolein as a lipid peroxidation product. *Trends Cardiovasc Med.* 1999;9(5):109-13.
33. Sayre LM, Lin D, Yuan Q, Zhu X, Tang X. Protein adducts generated from products of lipid oxidation: focus on HNE and ONE. *Drug Metab Rev*. 2006;38(4):651-75.
34. Forman H.J., Fukuto J.M., Miller T., Zhang H., Rinna A., Levy S. The chemistry of cell signaling by reactive oxygen and nitrogen species and 4-hydroxynonenal. *Arch. Biochem. Biophys*. 2008;477:183.
35. Higdon A., Diers A.R., Oh J.Y., Landar A., Darley-Usmar V.M. Cell signaling by reactive lipid species: new concepts and molecular mechanisms. *Biochem. J.*2012;442:453–464.
36. Poli G, Schaur RJ, Siems WG, Leonarduzzi G. 4-hydroxynonenal: a membrane lipid oxidation product of medicinal interest. *Med Res Rev*. 2008;28(4):569-631
37.Negre-Salvayre A, Auge N, Ayala V, Basaga H, et al. Pathological aspects of lipid peroxidation. *Free Radic Res*. 2010;44(10):1125-71.
38. Chapple SJ, Cheng X, Mann GE. Effects of 4-hydroxynonenal on vascular endothelial and smooth muscle cell redox signaling and function in health and disease. *Redox Biol*. 2013;1:319-31.
39. Santoso DI, Rogers P, Wallace EM, Manuelpillai U, Walker D, Subakir SB. Localization of indoleamine 2,3-dioxygenase and 4-hydroxynonenal in normal and pre-eclamptic placentae. *Placenta*. 2002;23(5):373-9.
40. Takagi Y, Nikaido T, Toki T, Kita N, Kanai M, Ashida T, Ohira S, Konishi I. Levels of oxidative stress and redox-related molecules in the placenta in preeclampsia and fetal growth restriction. *Virchows Arch*. 2004 ;444(1):49-55
41. Whitsett J., Picklo M.J., Sr, Vasquez-Vivar J. 4-Hydroxy-2-nonenal increases superoxide anion radical in endothelial cells via stimulated GTP cyclohydrolase proteasomal degradation. *Arteriosclerosis, Thrombosis, and Vascular Biology*. 2007;27:2340–2347.
42. Hattori Y., Hattori S., Kasai K. 4-hydroxynonenal prevents NO production in vascular smooth muscle cells by inhibiting nuclear factor-kappaB-dependent transcriptional activation of inducible NO synthase. *Arteriosclerosis Thrombosis and Vascular Biology*. 2001;21:1179–1183.
43. Shibata T, Shimozu Y, Wakita C, et al. Lipid peroxidation modification of protein generates Ne-(4-oxononanoyl)lysine as a pro-inflammatory ligand. *J. Biol. Chem*. 2011;286, 9943-19957.
44. Graham CH, Hawley TS, Hawley RG, et al. Establishment and characterization of first trimester human trophoblast cells with extended lifespan. *Exp Cell Res.*1993;206:204-11.
45. Manders EMM, Verbeek, FJ, Aten JA. Measurement of co-localization of objects in dual-colour confocal images. *Journal of Microscopy.* 1993;169, 375-382.

46. Zhu X, Gallogly MM, Mieyal JJ, et al. Covalent cross-linking of glutathione and carnosine to proteins by 4-oxo-2-nonenal. *Chemical Res. Toxicol*. 2009;22:1050–1059.
47. Perkins DN., Pappin DJC, Creasy DM, Cotrell JS. Probability-based protein identification by searching sequence databases using mass spectrometry data. *Electrophoresis* 1999;20:3551-3567.
48. Berman HM, Westbrook J, et al. The Protein Data Bank. *Nucleic Acids Res.*2000;28:235-242.
49. Pieper U, Webb BM, Dong GQ, et al. MODBASE, a database of annotated comparative protein structure models and associated resources. *Nucleic Acids Res*. 2014;42:D336-46.
50. Garcin ED, Bruns CM, Lloyd SJ, et al. Structural basis for isozyme-specific regulation of electron transfer in nitric-oxide synthase.*J.Biol.Chem*. 2004;279: 37918-37927.
51. Pettersen EF, Goddard TD, Huang CC, et al. UCSF Chimera--a visualization system for exploratory research and analysis *J. Comput. Chem*. 2004;25:1605-1612.
52. Xia C, Misra I, Iyanagi T, Kim JJ. Regulation of interdomain interactions by calmodulin in inducible nitric-oxide synthase. *J Biol Chem*. 2009;284:44, 30708-17.
53. Meng EC, Pettersen EF, Couch GS, et al. Tools for integrated sequence-structure analysis with UCSF Chimera. *BMC Bioinformatics*. 2006;7:339-349.
54.Li, H., Jamal, J., Plaza, C., Pineda, S.H., Chreifi, G., Jing, Q., Cinelli, M.A., Silverman, R.B., Poulos, T.L.Structures of Human Constitutive Nitric Oxide Synthases. *ActaCrystallogr*.,Sect.D2014;70: 2667.
55. Pensa, A.V., Cinelli, M.A., Li, H., Chreifi, G., Mukherjee, P., Roman, L.J., Martasek, P., Poulos, T.L., Silverman, R.B. Hydrophilic, Potent, and Selective 7-Substituted 2-Aminoquinolines as Improved Human Neuronal Nitric Oxide Synthase Inhibitors. *J. Med. Chem.*2017;60: 7146-7165.
56. Fedorova M, Griesser E, Vemula V, Weber D, Ni Z, Hoffmann R. Protein and lipid carbonylation in cellular model of nitrosative stress: mass spectrometry, biochemistry and microscopy study. *Free Radic Biol Med*. 2014;75 Suppl 1:S15.
57. Näsström T, Wahlberg T, Karlsson M, Nikolajeff F, Lannfelt L, Ingelsson M, Bergström J. The lipid peroxidation metabolite 4-oxo-2-nonenal cross-links α-synuclein causing rapid formation of stable oligomers. *BiochemBiophys Res Commun*. 2009;378;872-876.
58. Venema RC, Sayegh HS, Kent JD, Harrison DG. Identification, characterization, and comparison of the calmodulin-binding domains of the endothelial and inducible nitric oxide synthases. *J Biol Chem*;271(11):6435-40.
59. Zhang J, Martàsek P, Paschke R, et al. Crystal structure of the FAD/NADPH-binding domain of rat neuronal nitric-oxide synthase. Comparisons with NADPH-cytochrome P450 oxidoreductase. *J Biol Chem*. 2001;276(40):37506-13
60. Shimaoka M1, Iida T, Ohara A, et al. NOC, a nitric-oxide-releasing compound, induces dose dependent apoptosis in macrophages. *BiochemBiophys Res Commun*. 1995;209(2):519-26.
61. Krause BJ, Hanson MA, Casanello P. Role of nitric oxide in placental vascular development and function. *Placenta*. 2011;32(11):797-805
62. Matsubara K, Higaki T, Matsubara Y, Nawa A. Nitric oxide and reactive oxygen species in the pathogenesis of preeclampsia. *Int J Mol Sci*. 2015;16(3):4600-14.
63. Chen CA, Wang TY, Varadharaj S et al. S-glutathionylation uncouples eNOS and regulates its cellular and vascular function. *Nature*. 2010;468(7327):1115-8.
64. Doria E, Buonocore D, Focarelli A, Marzatico F. 2012. Relationship between human aging muscle and oxidative system pathway. *Oxid Med Cell Longev* 2012:830257.
65. Baraibar MA, Friguet B. 2012b. Oxidative proteome modifications target specific cellular pathways during oxidative stress, cellular senescence and aging. *Exp Gerontol* http://dx.doi.org/10.1016/j.exger.2012.10.007
66. Cindrova-Davies T, Fogarty NME, Jones CJP, Kingdom J, Burton GJ. Evidence of oxidative stress-induced senescence in mature, post-mature and pathological human placentas. *Placenta* 2018;68,15.
67. Hnat, M. D.; Meadows, J. W.; Brockman, D. E.; Pitzer, B.; Lyall, F.; Myatt, L. Heat shock protein-70 and 4-hydroxy-2-nonenal adducts in human placental villous tissue of normotensive, preeclamptic and intrauterine growth restricted pregnancies*. Am J ObstetGynecol*2005;193:836-840.

68. Rudra, C. B.; Qiu, C.; David, R. M.; Bralley, J. A.; Walsh, S. W.; Williams, M. A. A prospective study of early-pregnancy plasma malondialdehyde concentration and risk of preeclampsia. *Clin Biochem*200;39:722-726.
69. Watson AL, Palmer ME, Jauniaux E and Burton GJ. Variations in expression of copper/zinc superoxide dismutase in villous trophoblast of the human placenta with gestational age. *Placenta* 1997;18:295–299.
70. Doorn JA, Petersen DR. Covalent adduction of nucleophilic amino acids by 4-hydroxynonenal and 4-oxononenal*. Chem Biol Interact*. 2003;143-144:93-100.
71. Sharma NM, Patel KP. Post-translational Regulation of Neuronal Nitric Oxide Synthase: Implications for sympatho-excitatory states. *Expert OpinTher Targets*. 2017; 21(1): 11–22.
72. Du XL, Edelstein D, Dimmeler S, Ju Q, Sui C, Brownlee M. Hyperglycemia inhibits endothelial nitric oxide synthase activity by posttranslational modification at the Akt site.*J Clin Invest*. 2001;108(9):1341-8.
73. Lee SH, BlairIA. Characterization of 4-oxo-2-nonenal as a novel product of lipid peroxidation. *Chem. Res. Toxicol*. 2000;13:698–702.
74. Lin D, Lee HG, Liu Q, et al. 4-Oxo-2-nonenal is both more neurotoxic and more protein reactive than 4-hydroxy-2-nonenal. *Chem Res Toxicol*. 2005;18(8):1219-31.
75. Stewart BJ, Doorn JA, Petersen DR. Residue-specific adduction of tubulin by 4-hydroxynonenal and 4-oxononenal causes cross-linking and inhibits polymerization. *Chem. Res. Toxicol.*2007;20:1111-1119.
76. Galligan JJ, Rose KL, Beavers WN, Hill S, Tallman KA, Tansey WP, Marnett LJ. Stable histone adduction by 4-oxo-2-nonenal: a potential link between oxidative stress and epigenetics.*J Am Chem Soc.* 2014;136(34):11864-6
77. Novaro V, Colman-Lerner A, Ortega FV, Jawerbaum A, Paz D, Lo Nostro F, Pustovrh C, Gimeno MF, González E. Regulation of metalloproteinases by nitric oxide in human trophoblast cells in culture. *ReprodFertil Dev.* 2001;13(5-6):411-20.
78. Zhang X, Wang HM, Lin HY, Liu GY, Li QL, Zhu C. Regulation of matrix metalloproteinases (MMPS) and their inhibitors (TIMPS) during mouse peri-implantation: role of nitric oxide. *Placenta*. 2004 Apr;25(4):243-52.
79. Bolnick JM, Kilburn BA, Bolnick AD, Diamond MP, Singh M, Hertz M, Dai J, Armant DR.
Sildenafil stimulates human trophoblast invasion through nitric oxide and guanosine 3',5'-cyclic monophosphate signaling. *FertilSteril.* 2015;103(6):1587-95.e1-2.
80. Zhou Y, Fisher SJ, Janatpour M, Genbacev O, Dejana E, Wheelock M, Damsky CH. Human cytotrophoblasts adopt a vascular phenotype as they differentiate. A strategy for successful endovascular invasion? *J Clin Invest*, 99 (1997), pp. 2139-2151
81. Cartwright JE, Holden DP, Whitley GS. Hepatocyte growth factor regulates human trophoblast motility and invasion: a role for nitric oxide. *Br J Pharmacol*. 1999 Sep;128(1):181-9.
82. Lash GE, Warren AY, Underwood S, Baker PN. Vascular endothelial growth factor is a chemoattractant for trophoblast cells. *Placenta*. 2003;24(5):549-56.
83. Hinkle DE, Wiersma W, Jurs SG. Applied Statistics for the Behavioral Sciences. 5th ed. Boston: Houghton Mifflin; 2003.
84.Mukaka MM. Statistics corner: A guide to appropriate use of correlation coefficient in medical research. *Malawi Med J*. 2012;24(3):69–71.

Legends to the Figures

Figure 1. Protein carbonyl content and aldehyde-adduct accumulation in placentas

A, quantification of the protein carbonyl content (Enzo LifeSciences), in normal (n=4) and PE (n=4) placenta homogenates. Data are expressed as means ± SEM and statistical analysis was assessed using a Mann-Whitney test. **p<0.01

B,C, Immunofluorescence staining and confocal microscopy in normal (upper panels) and PE (lower panels) placentas, of acrolein- (left), HNE- (middle) and ONE- (right) adduct staining (in green), and nuclei DAPI staining (blue) (scale bar 20 µm), and chemical formulae of acrolein, HNE and ONE. The statistical quantification of adduct formation was expressed as fluorescence intensity *vs* DAPI staining. These pictures are representative of 4 control and 4 PE placentas separately analyzed. The data were expressed as medians with interquartile range and the statistical analysis was assessed using a Mann-Whitney test. *p<0.05.

Figure 2. eNOS is modified by LPO in PE placentas

Coimmunofluorescence staining and confocal microscopy in normal (left) and PE (right) placentas, of aldehyde-adduct (green), eNOS (red) and merge (yellow), and nuclei Dapi staining (blue) (scale bar 20 µm). Acrolein-adduct (upperpanels), HNE-adduct (HNE, middle panels), ONE-adduct (lower panel), and statistical quantification of adduct formation on eNOS for each aldehyde (middle graphes showing Pearson's coefficient or PCC, in front of each aldehyde/eNOS adduct detection). PCC measures the linear relationship between two signal intensities and allows to correlate the intensity distribution between the red channel (eNOS) and the green channel (aldehyde). We used the JACoP tool to analyse the Pearson's correlation coefficient [83,84].ONE-eNOS displayed the higher degree of colocalization (0.72 ± 0.09 *vs* 0.34 ± 0.10 for normal pregnancies), being closer to 1. Comparatively, HNE-eNOS colocalization was weaker (0.57 ± 0.02 vs 0.46 ± 0.05 for normal placentas) and acrolein-eNOS even lower (0.44 ± 0.02 vs 0.41 ± 0.02).

These pictures are representative of 4 control and 4 PE separately analyzed placentas. The data were expressed as medians with interquartile range and the statistical analysis was assessed using a Mann-Whitney test. *p<0.05; ns, non significant.

Figure 3. Recombinant eNOS modification by ONE

A, LC-MS/MS analysis of recombinant human eNOS (Enzo LifeScience). Recombinant eNOS (1 µg) was incubated overnight with ONE (1 mM). Mass spectrometric analysis identified 8 peptides with ONE modification. The fragment EPDNPK*$_{1085}$TYVQDILR had an experimental mass of 1822.95 while expected at 1686.847, and the fragment VK*$_{519}$ATILYGSETGR had an experimental mass of 1547.85

while expected at 1393.74. [1] measured mass of the modified peptide, [2] theoretical mass of the unmodified peptide. The percentage of modified peptide on total peptide was calculated for a given peptide, by comparing the area under the curve of the modified peptides *vs* total peptide, using Proline v2.0 software.

B, Enzymatic activity of recombinant eNOS modified by ONE (100 µM) and determined during 1h using the Nitric oxide Synthase activity assay kit (Abcam, France). The results are expressed as % of unmodified eNOS activity (control). The data were expressed as means ± SEM and the statistical analysis was assessed using a Student *t*-test. *p<0.05.

C, 3D-visualization of the oxygenase and reductase domains of eNOS, and putative location of ONE-modifiable Lys-residues. Left, oxygenase (heme) domain of human eNOS. The PDB structure 4D1O (chain A, cyan, clipped surface) was aligned with 5VVD (chain A, showing chains A and B of the crystal, purple). The Lysine residues are shown in orange (4D1O) at right (spheres) and the counterparts in 5VVD (chain B) are shown at left (sticks), as detailed in the Methods Section.

Right, reductase domains neuronal (Rat), endothelial (Human) and inducible (Human) NOS.

Combination of 3 aligned structures: Human eNOS (ModBase model 7e09b, Chain A: brown, clipped surface); Rat nNOS (PDB entry 1TLL, chain A: cyan, chain B: light-blue behind); Human iNOS (PDB entry 3HR4, chain A: yellow, aligned with 1TLL by chain A) complexed with calmodulin (3HR4, chain B: green, FMN ligand not shown). On the upper part of the picture, the domain 595-640 of eNOS(AI element) is depicted in purple. The ligands (FAD, FMN and NADPH with molecular surface) of 1TLL (used as template for ModBase model) are shown. The Lysine residues are shown in orange (ModBase model) (see details in the Method Section).

Figure 4. eNOS modification by ONE in HTR8 and effect on NO production

A, Representative pictures of ONE-Lys adduct colocalizing with eNOS in HTR8. Cells were incubated with ONE (1 µM, 2h at 37°C), then washed in PBS and fixed in 4% paraformaldehyde. The colocalization of eNOS and ONE-Lys adducts was studied in control untreated cells (upper panels) and in ONE-incubated cells (lower panels), by immunofluorescence and confocal microscopy as described in the Methods section (left, scale-bar 10 µm; right, scale-bar 5 µm).

B, Measurement of NO production by HTR8 and effect of ONE. HTR8 were preincubated with ONE (1 µM, 2h). DAF-FM diacetate probe (5µM) was added to the HTR8 culture medium 30 min before the end of the incubation. At the end, the medium was changed and the time-dependent production of NO was fluorometrically recorded (exc/em 495/525 nm) during 60 min. The results are expressed as arbitrary units of NO produced by control (black) and ONE-treated cells, means ± SEM of 3 separate experiments, statistical analysis with a Student *t*-test. **p<0.01

C, Measurement of eNOS activity in HTR8 preincubated for 2h with ONE (1 µM). After removing the

medium, cells were stimulated with VEGF (20 ng/mL, 15 min). The enzymatic activity of eNOS was performed on cell homogenate using the Nitric Oxide Synthase Assay Kit as described in the Methods Section.

Means ± SEM of 3 separated experiments, statistical analysis with a Student *t*-test. *p<0.05; ***p<0.001.

Figure 5. ONE inhibits the invasive capacity of HTR8. Protection by NOC-18

The wound-closure assay was done as described in the Methods Section. Confluent HTR8 were preincubated with ONE, in the conditions described in the legend to Fig.4. At the end, the medium was removed, and a scratch was made on confluent HTR8. Cells were maintained in hypoxia for 48h, in the absence or presence of the NO donor, NOC-18 (5 µM). After fixation, the slides were stained with DAPI and the migration of HTR8 into the wounded area was quantified. In A, representative images of HTR8 invasion and effect of NOC-18 in control hypoxia conditions (upper panels), and in HTR8 preincubated with ONE (lower panel). Scale bar = 100 µm. In B, quantification of cell having invaded the wound in each condition, and effect of NOC-18. Mean±SEM of 4 separate experiments, statistical analysis with a Student *t*-test. *p<0.05; ***p<0.001.

Figure 1

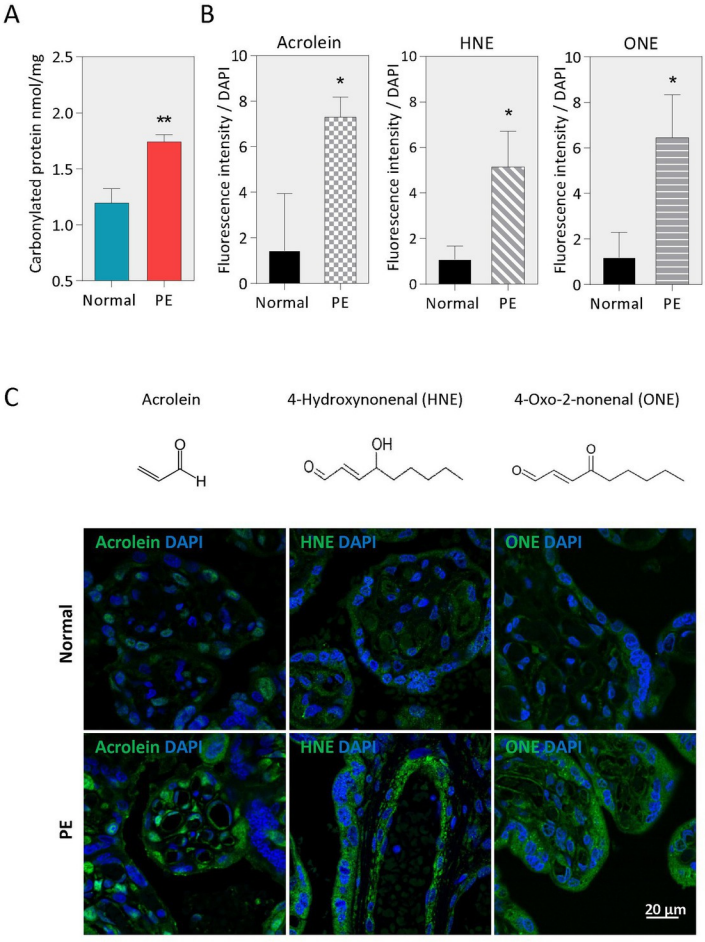
A
B
Carbonylated protein nmol/mg
2.5
2.0
1.5
1.0
0.5
**
Normal
PE
Acrolein
HNE
ONE
Fluorescence intensity / DAPI
10
8
6
4
2
0
*
Normal
PE
C
Acrolein
4-Hydroxynonenal (HNE)
4-Oxo-2-nonenal (ONE)
O
H
OH
Normal
PE
Acrolein DAPI
HNE DAPI
ONE DAPI
20 µm

Figure 2

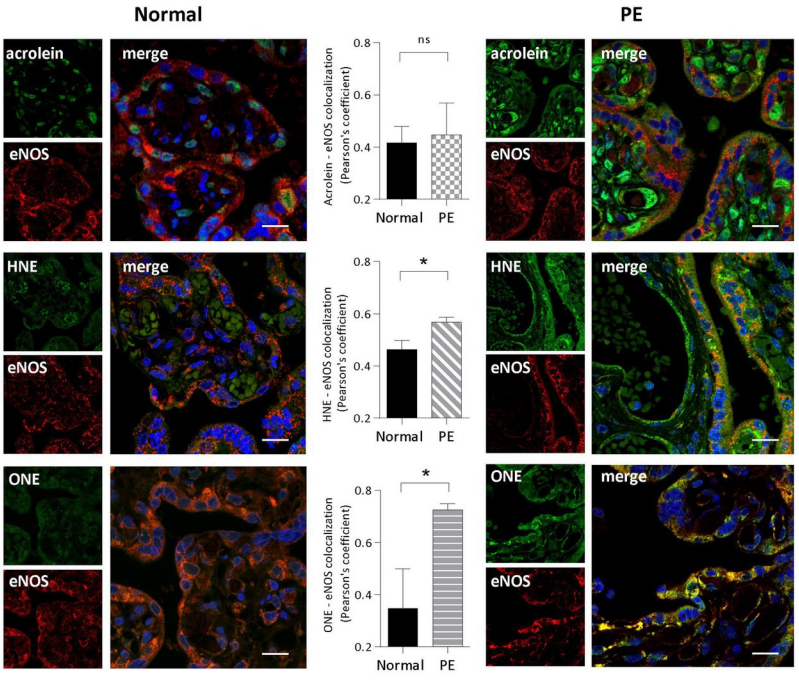
Normal
PE
acrolein
merge
eNOS
HNE
ONE
ns
*
*
Acrolein - eNOS colocalization (Pearson's coefficient)
HNE - eNOS colocalization (Pearson's coefficient)
ONE - eNOS colocalization (Pearson's coefficient)
0.8
0.6
0.4
0.2
Normal
PE

Figure 3

A

ONE-modified residues on recombinant human eNOS

Peptide	Modification	Modified residue	Experimental mass [1]	Expected mass [2]	P value	% modified peptide/ total peptide
SVENLQSSKSTR	4-ONE (K)	K773	1488.7806	1334.668	0.032	75.00%
VKATILYGSETGR	4-ONE (K)	K519	1547.8594	1393.746	0.0035	73.29%
KESSNTDSAGALGTLR	4-ONE (K)	K631	1759.8995	1605.785	0.0043	56.22%
EPDNPKTYVQDILR	4-ONE+Delta :H(-2)O(-1) (K)	K1085	1822.957	1686.847	0.0105	53.96%
DFINQYYSSIKR	4-ONE (K)	K139	1686.8683	1532.751	0.0066	47.74%
ESELVFGAKQAWR	4-ONE+Delta :H(-2)O(-1) (K)	K175	1655.8713	1519.767	2.40E-06	46.31%
VEDPPAPTEPVAVEQLE KGSPGGPPPGWVR	4-ONE (K)	K834	3245.672	3091.551	0.0112	37.31%
IQWGKLQVFDAR	4-ONE (K)	K192	1613.8969	1459.783	0.0039	29.58%

B

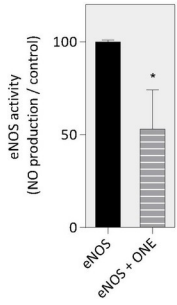

C

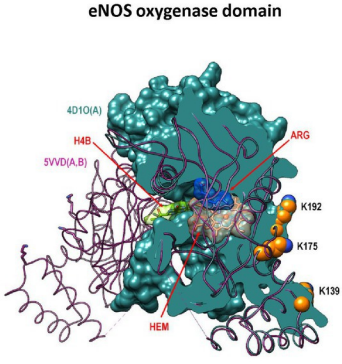

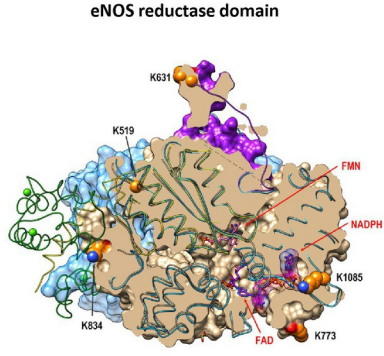

Figure 4

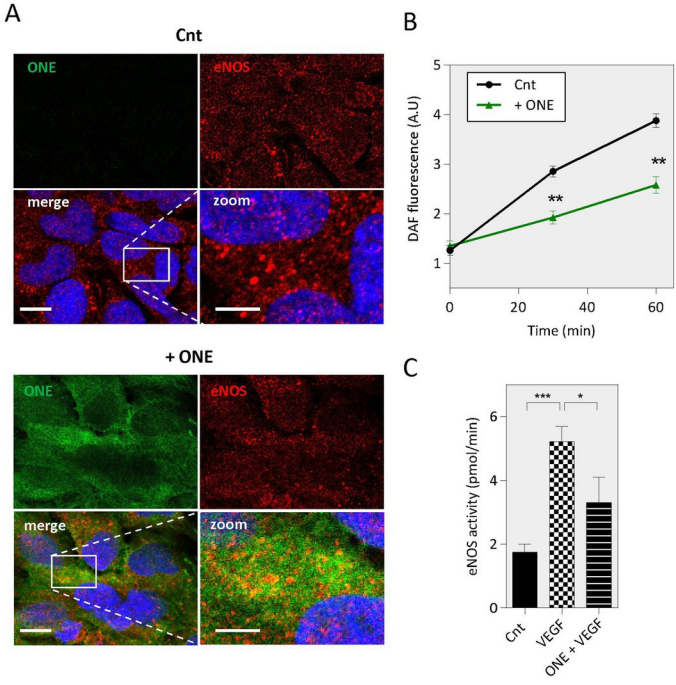
A
Cnt
ONE
eNOS
merge
zoom
+ ONE
ONE
eNOS
merge
zoom
B
Cnt
+ ONE
DAF fluorescence (A.U)
Time (min)
**
**
C
eNOS activity (pmol/min)
***
*
Cnt
VEGF
ONE + VEGF

Figure 5

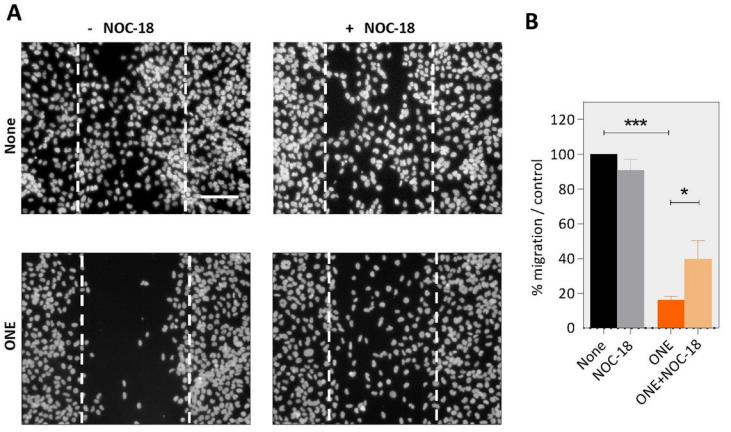
A
- NOC-18
+ NOC-18
None
ONE
B
% migration / control
120
100
80
60
40
20
0
***
*
None
NOC-18
ONE
ONE+NOC-18

Graphical abstract